AIAA 81-0616R

Response Characteristics of a Linear Rotorcraft Vibration Model

Donald L. Kunz*
U.S. Army Research and Technology Laboratories, (AVRADCOM), Ames Research Center, Moffett Field, Calif.

A fully coupled vibration model, consisting of a rotor with only flapping degrees of freedom plus pylon and fuselage pitching motion, was used in a parametric study undertaken to investigate the response characteristics of a simplified helicopter. Among the parameters studied were uncoupled body frequency, blade stiffness, hinge offset, advance ratio, and mast height. Results from the harmonic balance solution of the equations of motion show how each of these quantities affects the response of the model. The results also indicate that there is a potential for reducing vibration response through the judicious definition of the design parameters.

Nomenclature

a = blade airfoil lift curve slope
C_{M_4} = 4/rev pylon pitching-moment coefficient $= M_4/m\Omega^2R^3$
c = blade chord, m
E = Young's modulus, N/m^2
e = nondimensional hinge offset $= \epsilon/R$
H = mast height, m
h = nondimensional mast height $= H/R$
I = blade section area moment of inertia, m^4
I_B = blade mass moment of inertia $= mL^3/3$, kg-m^2
I_F = fuselage mass moment of inertia, kg-m^2
I_P = pylon mass moment of inertia, kg-m^2
I_R = rotor mass moment of inertia $= 2mR^3/3$, kg-m^2
k_θ = pylon/fuselage pitch spring stiffness, N-m/rad
L = blade length outboard of the hinge $= R-\epsilon$, m
M_4 = 4/rev pylon pitching moment, N-m
m = blade mass distribution, kg/m
R = rotor radius, m
V_0 = aircraft forward speed, m/s
β_{iP} = ith progressing flap mode
β_{iR} = ith regressing flap mode
γ = Lock number $= \rho acR^4/I_B$
ϵ = hinge offset, m
η = blade stiffness parameter $= (EI/m\Omega^2L^4)^{1/2}$
θ_c = longitudinal cyclic pitch angle, rad
θ_F/θ_P = pylon/fuselage pitch mode
θ_0 = collective pitch angle, rad
θ_s = lateral cyclic pitch angle, rad
$\ddot{\theta}_4^F$ = 4/rev fuselage pitch acceleration, nondimensionalized by Ω^2
μ = advance ratio $= V_0/\Omega R$
ρ = air density, kg/m^3
Ω = rotor speed, rad/s
ω = frequency, rad/s
ω_θ = uncoupled pylon/fuselage pitch frequency $= [k_\theta(I_P+I_F)/I_PI_F\Omega^2]^{1/2}$

Introduction

In recent years, there has been increased emphasis on reducing vibrations in rotorcraft. The need for such emphasis was brought sharply into focus during the competitions for the Army's Advanced Attack Helicopter (AAH) and Utility Tactical Transport Aircraft System (UTTAS). In both programs, the prototype aircraft had to undergo significant modifications because they did not meet vibration specifications. Even after they were modified, none of the aircraft could meet this requirement. As a result, the specifications were eventually relaxed so that they were more in line with the capabilities of current technology. The following facts indicate a serious gap in our understanding of vibrations in helicopters: 1) all of the prototypes had to be modified; 2) the vibration problems were only uncovered after they were flying; and 3) the Army inaccurately assessed related technology (as reflected in the original vibration requirement).

Research programs have been initiated by the government, industry, and academic community to investigate the phenomena that contribute to rotorcraft vibrations. Although the helicopter industry has been primarily concerned with incorporating new concepts and techniques into sophisticated programs that can be used for design and analysis, others have been working on specific aspects of the general problem. For example, Freeman and Wilson[1] use both theoretical and experimental techniques to investigate helicopter fuselage surface pressures that result from the main rotor flowfield. This study is particularly relevant to the problems encountered by both the AAH and UTTAS as a result of wake induced fuselage vibrations. Reference 2 is concerned with using the Vincent Circle method to modify a structure and reduce its vibration response. Both of these investigations neglect significant aspects of the complete vibration problem in order to concentrate on a specific phenomenon.

There is an approach to the study of rotorcraft vibrations that serves as an alternative to both the practice of using as much technology as possible to attack the problem in general and to that of conducting an intense investigation of an isolated aspect of the problem. This approach involves using a simple, but representative, model of the complete helicopter. Such a model is not sufficiently complex to permit precise results to be obtained, nor can it be used to study specific phenomena in detail. In can, however, be used as an aid to the understanding of the basic physical mechanisms governing helicopter vibrations. Investigations using simple models, such as those described in Refs. 3-5, have demonstrated the importance of the following factors: rotor-fuselage coupling, structural damping, flap modes higher than the first, interharmonic and intermodal coupling, and impedance modeling.

This investigation is intended as a follow-up to the work reported in Ref. 5. In that paper, the major emphases included the importance of properly coupling the rotor and fuselage, the effects of intermodal and interharmonic coupling, and the shortcomings of some of the traditional methods of avoiding vibration problems. Keeping in mind the lessons learned previously, we now look at how the

Presented as Paper 81-0616 at the AIAA Dynamics Specialists Conference, Atlanta, Ga., April 9-10, 1981; submitted April 24, 1981; revision received Sept. 7, 1981. This paper is declared a work of the U.S. Government and therefore is in the public domain.

*Research Scientist, Aeromechanics Laboratory. Member AIAA.

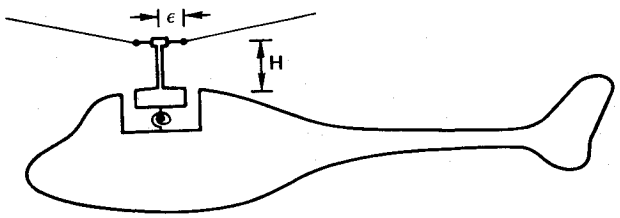

Fig. 1 Helicopter vibration model.

parameters that define the model affect its response and how they might be used to minimize the vibration levels.

Mathematical Model and Analysis

Like the mathematical model used in Ref. 5, this model is a subset of QUIVR (Qualitative Investigation of Vibrations in Rotorcraft). The major difference between the two is that the model discussed herein has an articulated rotor; the rotor in the previous model was hingeless. This alteration was made primarily so that the influences of hinge offset and blade stiffness could be analyzed separately. In addition, mast height has been included in this investigation. A schematic of the model is shown in Fig. 1.

Each of the four blades in the rotor is uniform and hinged at a distance ϵ outboard of the center of rotation. The flapping deflections outboard of the hinge are represented by three mode shapes: one rigid blade mode and two pinned-free modes. In addition to allowing us to separate the effects of hinge offset and blade stiffness, this blade representation is valid down to zero blade stiffness. This was not the case for hingeless blades using cantilever mode shapes. As in Ref. 5, the blade aerodynamic forces come from a quasi-steady strip theory analysis in which stall, compressibility, reversed flow, and apparent mass effects are neglected. The aircraft is assumed to be in steady, level, forward flight.

The pylon is a nonrotating rigid body which has its mass center located a distance H directly below the hub center of rotation. For most configurations considered here, H is taken to be zero. It is assumed that the pylon has only the pitching degree of freedom in this investigation. The fuselage is also a rigid body, and its mass center is coincident with the pylon center of mass. It is also constrained to have only pitching rotations. The pylon and fuselage are connected to one another through rotational springs located at the interface of the pylon and fuselage.

Numerical considerations within the computer program that performs this analysis dictate that a small amount of damping (0.01% critical) be included at the pylon/fuselage interface. In addition, extremely soft springs have been inserted to provide a ground connection for the fuselage. These modifications to the model ensure that the system matrices are invertible; they do not result in any significant changes in the solutions.

The vibration response of the mathematical model is obtained through the harmonic balance method,[6] which transforms the differential equations of motion into algebraic equations and solves for the Fourier coefficients of each generalized coordinate. These harmonic components of the response are then used to solve for the resultant shears and moments on the pylon at the base of the mast. When the mast height is zero, these are the hub shears and moments. In addition to the responses of each coordinate and the pylon loads, the eigenvalues of the system in a vacuum and/or in the air can also be obtained. Because of the periodic coefficients of the equations, the constant coefficient approximation is used in computing the eigenvalues in air.

Results and Discussion

To assess the influence of the parameters that define the mathematical model described above, the values of these parameters were varied individually or in pairs. The parameters that were not being investigated were maintained at their nominal values (Table 1) unless otherwise noted. The results of this study are discussed in the following paragraphs.

Table 1 Nominal values of the model parameters

Parameter	Nominal value
ω_θ	3.0
η	0.05
e	0.05
I_R/I_P	5.0
I_F/I_P	40.0
h	0.0
μ	0.2
γ	8.0
Ω	30 rad/s
R	7.62 m
m	11.97 kg/m

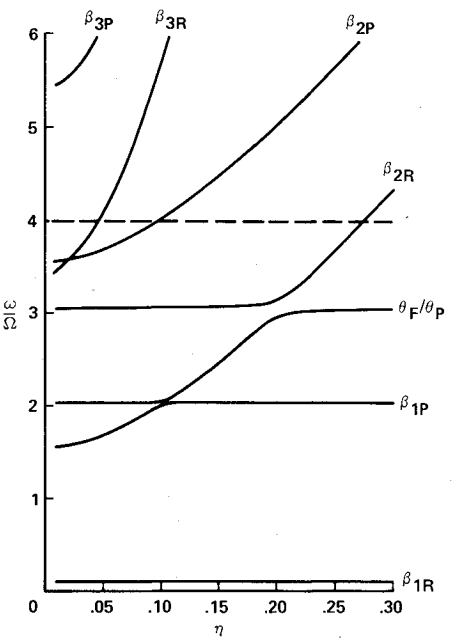

Fig. 2 Vacuum eigenvalues as a function of blade stiffness.

Blade Stiffness and Hinge Offset

In Ref. 5, the rotor blades were cantilevered at the hub center of rotation. Although this hingeless rotor configuration is attractive because of its simplicity and because of the increased control power that it provides, studies of the configuration do not allow the analyst to separate the effect of blade stiffness from the effect of hinge offset. In this investigation, we consider an articulated rotor in order to clarify this issue.

Figures 2 and 3 are plots of the coupled eigenvalues of the vibration model for variations in the values of blade stiffness and hinge offset, respectively. The first difference between the effects of these two parameters can be seen by comparing these figures. In Fig. 2 we see that changes in blade stiffness have no effect on the first flapping mode frequencies, but significantly alter the frequencies of the higher modes. This is, of course, to be expected, since the first flapping mode shape of a hinged blade is nearly a straight line, so both the mode shape and frequency are virtually unaffected by stiffness changes. It should also be noted that although Fig. 2 shows values of blade stiffness up to $\eta = 0.3$, only rarely do blades have stiffnesses greater than $\eta = 0.1$. Figure 3 demonstrates that all of the blade modal frequencies are altered by changes

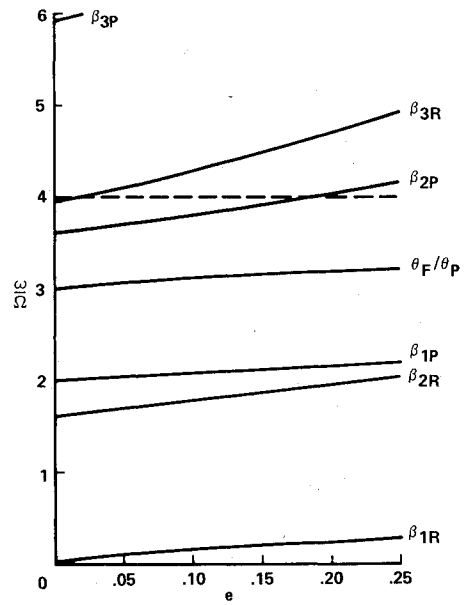

Fig. 3 Vacuum eigenvalues as a function of hinge offset.

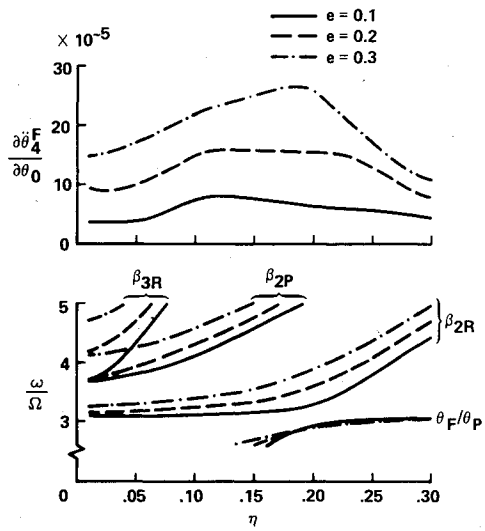

Fig. 4 Effects of blade stiffness and hinge offset on the fuselage response derivative and the coupled natural frequencies (in vacuo).

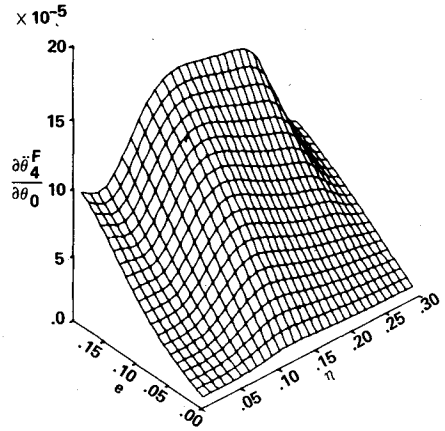

Fig. 5 Surface plot of the fuselage response derivative as a function of blade stiffness and hinge offset.

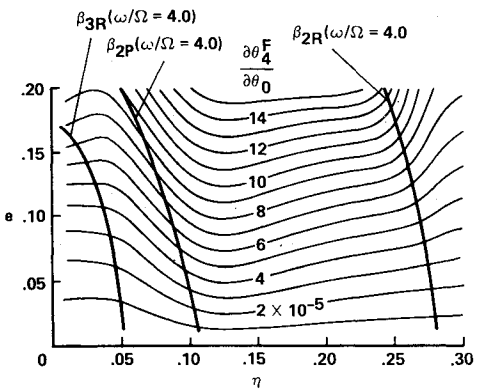

Fig. 6 Contour plot of the fuselage response derivative as a function of blade stiffness and hinge offset (4/rev vacuum eigenvalues superimposed).

in hinge offset. However, the effect on modes higher than the first is much less than that resulting from stiffness changes.

Another way in which the hinge offset affects the system is illustrated in Fig. 4. In the lower portion of the figure, where the coupled eigenvalues are plotted for three values of hinge offset, we see that as e increases, the coupling between the modes labeled β_{2R} and θ_F/θ_P becomes stronger. If β_{2R} and θ_F/θ_P were uncoupled, the θ_F/θ_P mode would have a constant frequency of $\omega/\Omega = 3.0$ for all η, and β_{2R} would simply intersect the θ_F/θ_P mode. With coupling, the modes change character as their frequencies approach one another. The mode, which can be identified as the second regressing flap mode at $\eta = 0.30$, starts out at $\eta = 0.01$ as the pylon/fuselage pitch mode. As η increases past $\eta = 0.15$ (for $e = 0.1$), the mode begins to change composition until it becomes primarily a blade flapping mode near $\eta = 0.25$. For larger values of e, the change is more gradual and encompasses a larger part of the η range. The reason for this behavior is that the coupling between the modes is increasing with e. The increase in coupling is in turn a result of the fact that larger hinge offsets allow larger moments to be transmitted between the rotor and fuselage.

The top portion of Fig. 4 shows the fuselage 4/rev response for the same variation in η as in the lower half of the figure. Note that as the hinge offset, and hence the coupling, increases, the response peak caused by the excitation of the β_{2R} mode becomes more pronounced. This is most likely because the body pitch motion contributes more to the regressing flap mode as the coupling gets stronger.

In Fig. 5, the fuselage vibration response derivative is plotted against both hinge offset and blade stiffness. It can readily be seen that for a given blade stiffness η, the response will increase with hinge offset. For most configurations, the response will show a monotonic increase as the hinge offset is increased.

Although a surface plot like that in Fig. 5 is useful in quickly locating the ranges of maximum and minimum response, a contour map of the surface can also be valuable in interpreting the results. Figure 6 is a contour map of Fig. 5, with the locus of eigenvalues equal to 4.0 superimposed on it. Using both figures, it can be seen that the two maxima running nearly parallel to the e-axis result from second progressing and regressing flap modes being excited. Note also that the presence of the third regressing flap mode has little effect on the response of the fuselage.

Since the contours of Fig. 6 indicate curves of constant response, the blade stiffness and hinge offset can be changed with no attendant change in response, as long as the new design point remains on the same contour line. It is therefore possible to increase the hinge offset and obtain increased control power, as long as the response is not already in a region of minimum response. For example, let us assume that a blade has been designed with a 5% hinge offset and a stiffness of $\eta = 0.1$ (the first and second flapping frequencies

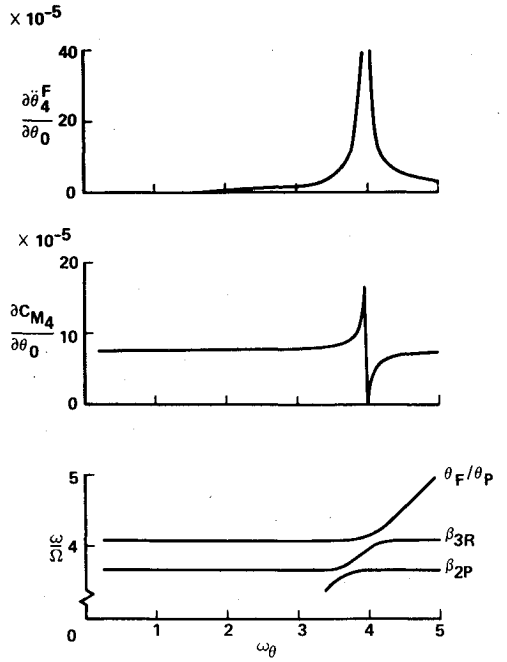

Fig. 7 Fuselage response, pitching moment, and vacuum eigenvalues as function of pylon/fuselage frequency.

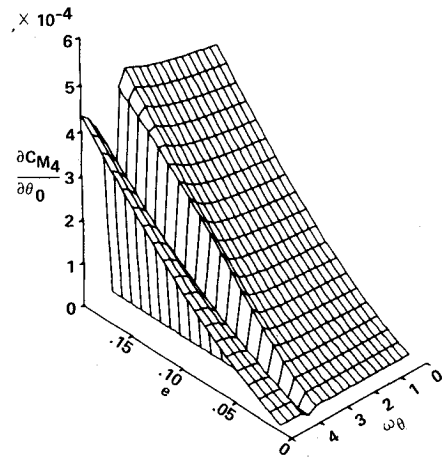

Fig. 8 Surface plot showing the effects of hinge offset and pylon/fuselage frequency on the pitching moment derivative.

would be approximately 1.02 and 3.02, respectively). From Fig. 6, it would be possible to increase the hinge offset, while simultaneously decreasing the blade stiffness, without increasing the fuselage response. In fact, for somewhat smaller increases in hinge offset and larger decreases in stiffness, the response could be reduced.

Body Frequency and Hinge Offset

The effect of the uncoupled pylon/fuselage natural frequency on the fuselage pitching response, on the pylon pitching moment, and on the system natural frequencies is shown in Fig. 7. Both Refs. 3 and 5 discuss this phenomenon, which occurs in the vicinity of $\omega_\theta = 4.0$. Briefly, the pitching moment goes to zero at $\omega_\theta = 4.0$ because the transfer function for the uncoupled pylon and fuselage requires that any small pitching moment result in an infinite response. Since the coupled system natural frequency at $\omega_\theta = 4.0$ is not exactly equal to 4.0, the undamped system response must be finite, forcing the pitching moment to zero at $\omega_\theta = 4.0$. For the configuration analyzed in Fig. 7, the coupled system natural frequency is equal to 4.0 near $\omega_\theta = 4.05$, and the peak fuselage response occurs near $\omega_\theta = 3.95$.

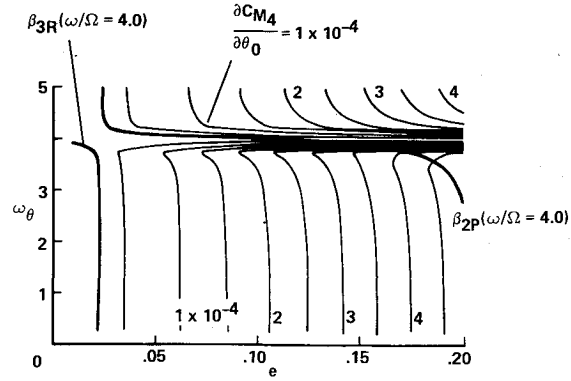

Fig. 9 Contour plot showing the effects of hinge offset and pylon/fuselage frequency on the pitching moment derivative (4/rev vacuum eigenvalues superimposed).

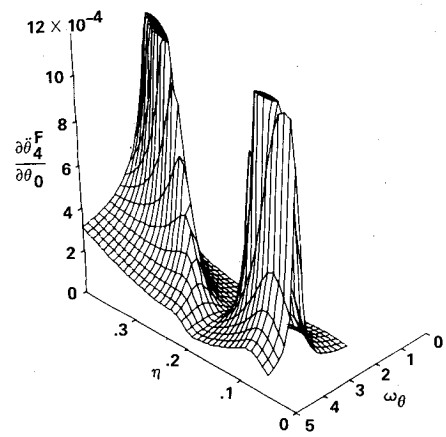

Fig. 10 Surface plot of the fuselage response derivative as a function of blade stiffness and pylon/fuselage frequency for a hingeless rotor (from Ref. 5).

As discussed previously, increasing the hinge offset strengthens the coupling between the pylon/fuselage mode and the blade flapping modes. In Fig. 8, it can be seen that the location of the peak pitching moment is also affected. Because of the grid size in Fig. 8, the exact location of the peak cannot be determined; however, it can be seen that it is occurring at smaller values of ω_θ as the hinge offset increases. Figure 9, which is a contour plot of Fig. 8, shows that not only does peak moment occur at smaller ω_θ as e increases, but those locations for which the system natural frequency equals 4.0 behave similarly.

Blade Stiffness and Body Frequency

One of the more interesting features of the results presented in Ref. 5 was the pronounced minimum in the fuselage response for a hingeless rotor that occurred near $\eta = 0.2$ and extended over the entire range of body frequency (Fig. 10). Since that investigation used only hingeless rotors, any increase in the blade stiffness was accompanied by an increase in the effective hinge offset. By using an articulated rotor in this study, the effectiveness of modeling a hingeless blade with an articulated blade having an appropriate hinge offset could be examined. Also, by separating the effects of blade stiffness and hinge offset, the source of the response minimum might be determined.

From Figs. 5 and 8, it is apparent that hinge offset changes alone cannot explain the phenomenon. Turning then to Fig. 11, which shows the fuselage vibration response for an articulated rotor subject to variations of ω_θ and η, we can see no minimum region as pronounced as that in Fig. 10. There is, however, a somewhat less notable region near $\eta = 0.27$. One

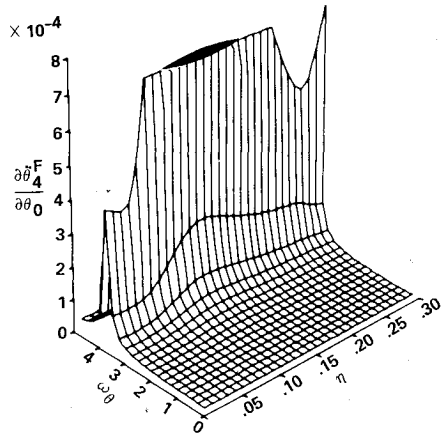

Fig. 11 Surface plot of the fuselage response derivative as a function of blade stiffness and pylon/fuselage frequency.

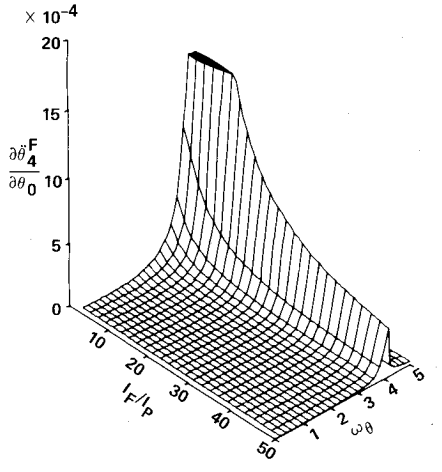

Fig. 12 Surface plot showing the effect of inertia ratio on the fuselage response derivative over a range of pylon/fuselage frequencies.

might conjecture that this minimum would correspond more closely to that in Fig. 10 if the hinge offset were larger. After all, for a hingeless blade, $\eta = 0.2$ implies a rather large effective hinge offset. However, we have already seen that increasing e only increases the response (Fig. 5). We must conclude, therefore, that the phenomenon illustrated in Fig. 10 cannot be adequately modeled using an articulated rotor. Further, it appears likely that no one parameter is the source of this result; instead, it is a combination of parameters that determines the character of the mode that is being excited.

Inertia Ratio

It is obvious that if a helicopter fuselage had an infinite pitch inertia, the fuselage pitch response would be zero. Although this would solve the problem of vibrations, it would hardly be a practical solution. It is, however, practical to look at the ratio of the fuselage inertia to the pylon inertia within a reasonable range of values. Since it is the fuselage inertia that is being varied while the pylon inertia is held constant, the inertia ratio is a measure of the aircraft's "unsprung" fuselage inertia to its "sprung" pylon inertia.

As Fig. 12 demonstrates, the pitch response decreases as the inertia ratio increases for all values of pylon/fuselage natural frequency. Therefore it might be advantageous for a designer to look at decreasing the inertias of the "sprung" masses as a means of reducing fuselage response. Another approach would be to investigate a means for having a smaller part of the pylon structure supported by springs. Perhaps this could be accomplished by rigidly attaching the transmission to the fuselage, supporting the mast on springs, and using flexible couplings in the rotor drive shaft.

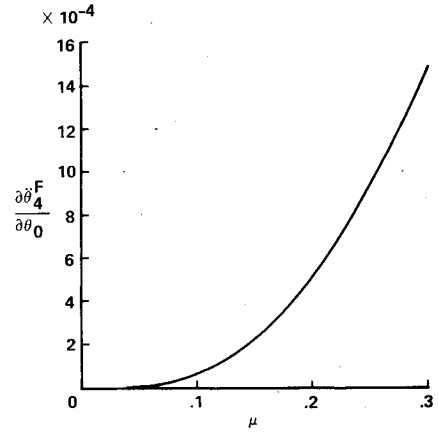

Fig. 13 Effect of advance ratio on the fuselage response derivative.

Advance Ratio

It is well known that the vibration response of helicopters is a strong function of forward speed. The curve in Fig. 13 shows the fuselage pitch response obtained from QUIVR over a range of advance ratios. One immediately observes that the curve is approximately quadratic over the entire range of values. Also, the typical increase in response through the low-speed, transition flight regime is not present. Both of these results are consequences of the aerodynamic model that was selected for this analysis.

In this quasi-steady aerodynamic model, all of the terms containing advance ratio are either linear or quadratic in that quantity. Thus it should come as no surprise that the response is a quadratic function of advance ratio. The increase in response during transition is generally regarded as being related to the unsteady flowfield around the rotor. In transition, the wakes shed by the blades are very near the rotor and interact with the passing blades to produce increased rotor loads. The aerodynamic model used in this analysis does not include a wake model and therefore cannot be expected to model the transition response. In spite of this deficiency, the analysis does very well in the moderate-speed region between transition and high-speed flight. As shown in Ref. 7, the response at moderate advance ratios does appear to be quadratic in μ.

Mast Height

In the development of both the UTTAS and AAH it was necessary to raise the rotors (i.e., increase the mast height) in order to reduce the level of vibration. The rationale behind this solution was that the vibration was being caused by the impingement of the rotor wake pressure waves on the fuselage, and that raising the rotor would provide time for some of the wake's energy to dissipate before the pressure waves reached the fuselage. In addition, the raised rotor would reduce the interference between the fuselage and rotor flowfields, which was thought to be a source of vibration. Since this analysis contains no wake model, the wake impingement on the fuselage could not be investigated. However, the raising of the rotor will affect the response in ways not related to the wake aerodynamics (e.g., rotor/body dynamics). With this analysis, some of these effects can be investigated.

One obvious result of increasing the mast height is that the overall pitching inertia of the aircraft will be increased. As shown in Fig. 14, the frequency of the pylon/fuselage pitching mode decreases as the mast height increases. This is, of course, a natural result of the increased inertia of the aircraft. As before, the pylon/fuselage modes couple with rotor modes as their frequencies converge.

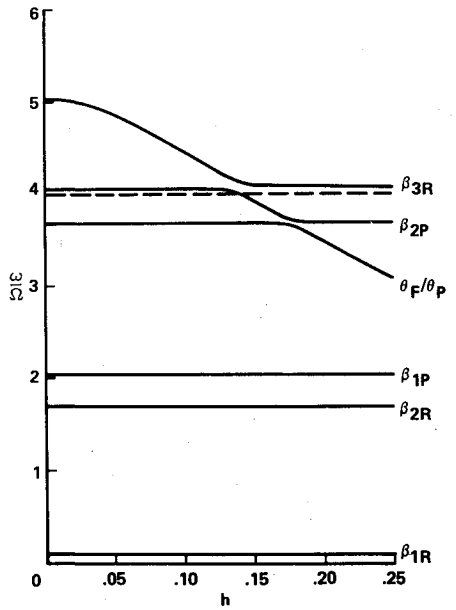

Fig. 14 Vacuum eigenvalues as a function of mast height; $\omega_\theta = 5.0$.

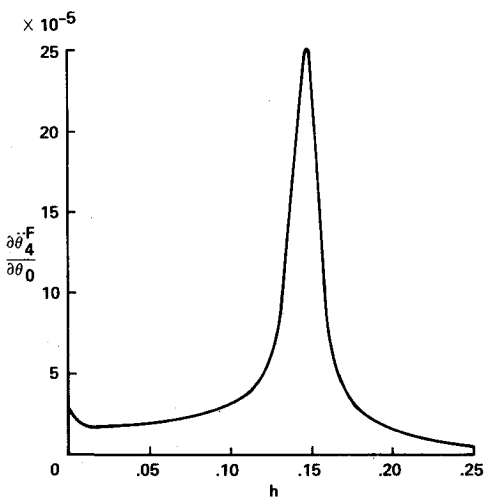

Fig. 15 Fuselage response derivative as a function of mast height; $\omega_\theta = 5.0, \theta_0 = \theta_c = \theta_s = 0$.

In all of the configurations considered thus far, the mast height has been zero and the moment and response derivatives have been independent of the control settings (θ_0, θ_c, θ_s). This is not merely a coincidence. If we consider the pylon and fuselage to be pitching about a point, the rotor hub motion can be broken out into three components: pitching motion, fore-and-aft motion (if the mast height is nonzero), and plunging motion (which can be neglected because of the assumption of small angles). From the point of view of the rotor blades, the hub pitching motion is equivalent to cyclic flapping of the blades and the fore-and-aft motion is equivalent to cyclic in-plane blade motion. Since blade flapping is already included in the model, the only terms added to the equations of motion by the hub pitching motion are those that are analogous to the blade flapping terms already there. The fore-and-aft hub motion, however, introduces terms analogous to the ones that would be present if in-plane blade motions had been included. Among these terms are aerodynamic terms that are functions of the control parameters. The blade flapping terms are not functions of the control variables because θ_0, θ_s, and θ_c are assumed to be small angles (cosine effect). Therefore, when the mast height in nonzero, the moment and response derivatives are also functions of θ_0, θ_c, and θ_s.

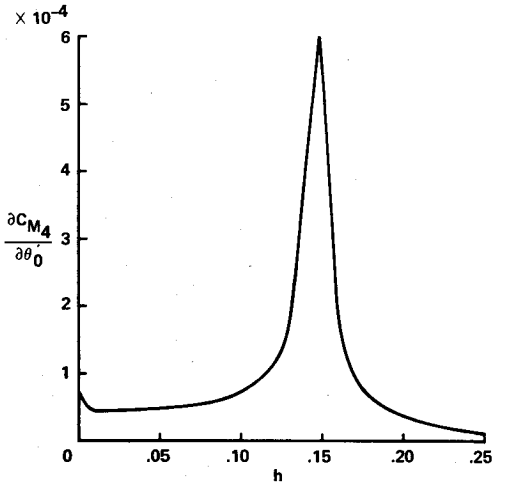

Fig. 16 Pitching moment derivative as a function of mast height; $\omega_\theta = 5.0, \theta_0 = \theta_c = \theta_s = 0$.

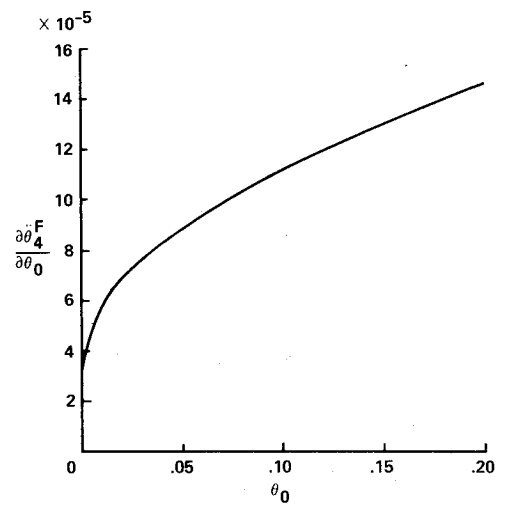

Fig. 17 Effect of collective pitch angle on the fuselage response derivative; $\omega_\theta = 5.0, h = 0.1, \theta_c = \theta_s = 0$.

Figure 15 is a plot of the 4/rev pitching response derivative vs mast height. The sharp peak near $h = 0.15$ roughly corresponds to the location in Fig. 14 where the coupled pylon/fuselage pitch mode frequency equals 4/rev. It should be noted, however, that this is not the same phenomenon that was illustrated in Fig. 7. As indicated in Fig. 16, at no time does the pitching moment approach zero, nor is there any significant difference in the shapes of the curves in Figs. 15 and 16. Therefore it is apparent that the fuselage transfer function does not require an infinite response for any finite moment at any point within this range of values for mast height. In fact, the only time when this will occur is when $\omega_\theta = 4.0$.

To see how variations in the collective pitch affect the magnitude of the fuselage response derivative when the mast height is greater than zero, we turn to Fig. 17. Here, for $h = 0.1$, it can be seen that the response increases rapidly as the pitch angle increases from zero. At higher angles, the slope of the curve decreases, indicating that the most pronounced changes in response will occur near $\theta_0 = 0$. In addition to affecting the magnitude of the fuselage response, variations in collective pitch also cause shifts in the location of the response peak with respect to h. As we can see from Fig. 18, in which the model parameters are identical to those in Fig. 15 (except that θ_0 has been increased from 0.0 to 0.1), the peak response has shifted from $h = 0.15$ (Fig. 15) to $h = 0.17$. This figure also shows a change in the shape of the peak in comparison with

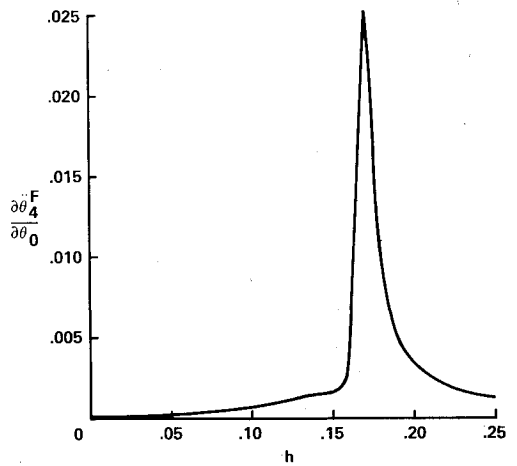

Fig. 18 Fuselage response derivative as a function of mast height; $\omega_\theta = 5.0, \theta_0 = 0.1, \theta_c = \theta_s = 0$.

that of Fig. 15. Thus it can be seen that when selecting the mast height for minimum vibration, one must consider the flight condition of the aircraft.

Summary

A parametric study was performed to assess the ways in which the various quantities that define a simple rotorcraft model influence the vibration response of the model system. Since any analysis in which the rotor is uncoupled from the pylon/fuselage cannot produce accurate results, even for a simple model such as this, a model that rigorously couples the rotor to the pylon and fuselage was used. The major observations from this investigation are as follows:

1) Increasing the hinge offset allows larger moments to be transmitted between the rotor and pylon/fuselage. This increases the strength of the coupling between the rotor and body modes and, in general, increases the magnitude of the response.

2) An increase in control power obtained by using a larger hinge offset is not necessarily accompanied by an increase in vibratory response, if the blade stiffness can be properly adjusted. Conversely, a decrease in vibration may be obtained, without adversely affecting the control power, by altering the blade stiffness.

3) The response characteristics of a hingeless rotor and an articulated rotor have some fundamental differences. Although a hingeless rotor has an effective hinge offset, its response characteristics cannot be completely duplicated using an articulated rotor. It is likely that these differences result from the differences in the shapes of the modes being excited.

4) One can decrease the vibratory response of a helicopter by increasing the ratio of the inertia of the fuselage structure to the inertia of the structure on springs above the fuselage.

5) For this mathematical model, nonzero mast heights cause the moment and response derivatives to become functions of the control variables. This is a result of the fact that with a finite mast height, the pitching motion of the pylon causes a fore-and-aft motion of the rotor that is analogous to adding a cyclic in-plane rotor degree of freedom.

6) When the mast height is greater than zero, the pitch angle has a significant effect on the moment and response derivatives. Not only do these derivatives increase in magnitude with pitch angle, but the peaks also shift to other values of mast height.

References

[1] Freeman, C.E. and Wilson, J.C., "Rotor-Body Interference (ROBIN) Analysis and Test," *Proceedings of the 36th Annual Forum of the American Helicopter Society,* Washington, D.C., May 1980.

[2] Done, G.T.S. and Hughes, A.D., "The Response of a Vibrating Structure as a Function of Structural Parameters," *Journal of Sound and Vibration,* Vol. 38, Feb. 1975, pp. 255-266.

[3] Hohenemser, K.H. and Yin, S.-K., "The Role of Rotor Impedance in the Vibration Analysis of Rotorcraft," *Vertica,* Vol. 3, No. 3/4, 1979, pp. 189-204.

[4] Hsu, T.-K. and Peters, D.A., "Coupled Rotor/Airframe Vibration Analysis by a Combined Harmonic-Balance, Impedance-Matching Method," *Proceedings of the 36th Annual Forum of the American Helicopter Society,* Washington, D.C., May 1980.

[5] Kunz, D.L., "Effects of Rotor-Body Coupling in a Linear Rotorcraft Vibration Model," *Proceedings of the 36th Annual Forum of the American Helicopter Society,* Washington, D.C., May 1980.

[6] Peters, D.A. and Ormiston, R.A., "Flapping Response of Hingeless Rotor Blades by a Generalized Harmonic Balance Method," NASA TN D-7856, Feb. 1975.

[7] Schrage, D.P. and Peskar, R.E., "Helicopter Vibration Requirements," *Proceedings of the 33rd Annual Forum of the American Helicopter Society,* Washington, D.C., May 1977.